RESEARCH ARTICLE | JANUARY 30 2023

Modified magnetism in heterostructures of $Cr_2Ge_2Te_6$ and oxides

A. E. Llacsahuanga Allcca; H. Idzuchi ✉; X. C. Pan; ... et. al

AIP Advances 13, 015031 (2023)
https://doi.org/10.1063/9.0000413

Modified magnetism in heterostructures of $Cr_2Ge_2Te_6$ and oxides

Cite as: AIP Advances 13, 015031 (2023); doi: 10.1063/9.0000413
Submitted: 1 October 2022 • Accepted: 9 November 2022 •
Published Online: 30 January 2023

A. E. Llacsahuanga Allcca,[1] H. Idzuchi,[1,2,3,4,a)] X. C. Pan,[2] K. Tanigaki,[2,5] and Y. P. Chen[1,2,3,6,7,b)]

AFFILIATIONS

[1] Department of Physics and Astronomy, Purdue University, West Lafayette, Indiana 47907, USA
[2] WPI Advanced Institute for Materials Research (AIMR), Tohoku University, Sendai 980-8577, Japan
[3] Center for Science and Innovation in Spintronics (CSIS), Tohoku University, Sendai 980-8577, Japan
[4] Department of Physics, The University of Tokyo, Bunkyo-ku, Tokyo 113-0033, Japan
[5] Beijing Academy of Quantum Information and Sciences, Haiden District, Beijing 100193, China
[6] School of Electrical and Computer Engineering and Birck Nanotechnology Center and Purdue Quantum Science and Engineering Institute, Purdue University, West Lafayette, Indiana 47907, USA
[7] Institute of Physics and Astronomy and Villum Centers for Dirac Materials and for Hybrid Quantum Materials and Devices, Aarhus University, 8000 Aarhus-C, Denmark

Note: This paper was presented at the 67th Annual Conference on Magnetism and Magnetic Materials.
[a)] **Author to whom correspondence should be addressed:** idzuchi@g.u-tokyo.ac.jp
[b)] yongchen@purdue.edu

ABSTRACT

We study the effects of interfacing the van der Waals ferromagnet $Cr_2Ge_2Te_6$ with oxide layers, such as NiO and MgO, in a few different configurations. For this, the magnetic hysteresis curves, obtained by magneto optical Kerr effect, of $Cr_2Ge_2Te_6$ flakes of similar thicknesses were evaluated. Compared to the properties of a bare $Cr_2Ge_2Te_6$, we observed an increased perpendicular magnetic anisotropy and enhanced Curie temperature in the $Cr_2Ge_2Te_6$/NiO heterostructure. In contrast, we report little or no change of the magnetic properties in a $Cr_2Ge_2Te_6$/NiO and $Cr_2Ge_2Te_6$/MgO where the $Cr_2Ge_2Te_6$ was exfoliated on top of the oxide layer. Finally, strain is considered as the mechanism of the enhancement, as we observed the formation of wrinkles in thin $Cr_2Ge_2Te_6$/NiO heterostructure and the Raman characteristics close to the wrinkles indicated a tensile strain, which is consistent with stronger ferromagnetism in $Cr_2Ge_2Te_6$.

In recent years, the discovery of two-dimensional magnetism in layered materials[1–3] has expanded the growing repertoire of van der Waals layered compounds, adding magnetism as a new degree of freedom to engineer functionality into heterostructures built from these compounds. It has triggered a rapid development of techniques to modify their magnetism to make them more appealing for technological applications. However, the ferromagnetic transition temperature (Curie temperature, T_C) remains relatively low so far (especially for magnetic insulators): the T_C for monolayer CrI_3 (45 K) and bilayer $Cr_2Ge_2Te_6$ (30 K) are even lower than their bulk counterparts (61 K and 66 K for bulk CrI_3 and bulk $Cr_2Ge_2Te_6$ respectively) and required cryogenic techniques to reach.[1,2] Therefore, great effort in enhancing their T_C has been attempted including techniques such as electrostatic doping,[4–8] ion intercalation[9] and interface engineering.[10,11] The interface engineering takes advantage of many unexplored interface properties of van der Waals materials. We have reported earlier the increase of Curie temperature nearly two-fold and an enhanced perpendicular anisotropy for $Cr_2Ge_2Te_6$/NiO, yet, the microscopic mechanism of the change of the magnetic properties remained elusive.[12] Here, we report the magnetism and characterization related to the system of $Cr_2Ge_2Te_6$/NiO and investigate a possible mechanism of the enhanced magnetism.

We studied $Cr_2Ge_2Te_6$ (CGT) as layered ferromagnet with mechanical cleavability down to atomically thin layers. The crystal was synthetized in its crystal form via the self-flux technique. Briefly, 100 mg of Cr powder, 200 mg of Ge powder and 2 g of Te were

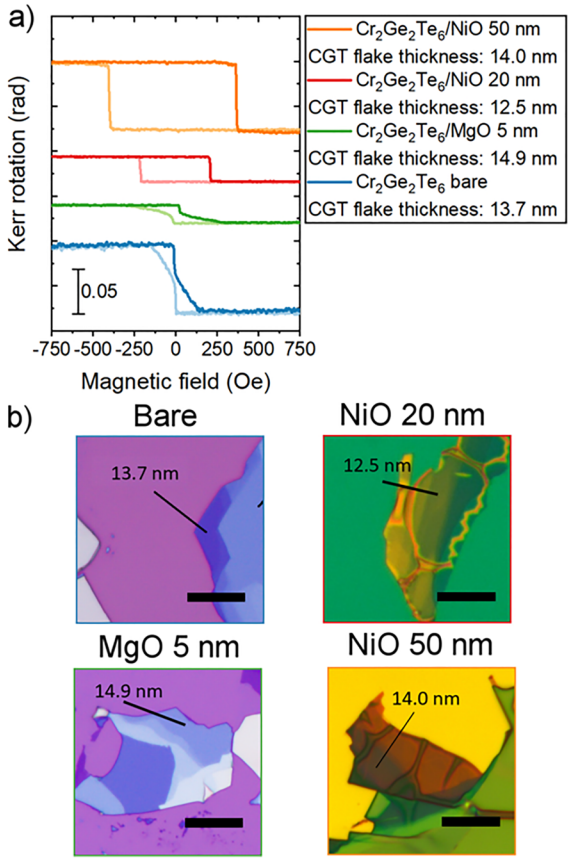

FIG. 1. (a) Magneto optical Kerr effect (MOKE) curves at the temperature of 7 K of $Cr_2Ge_2Te_6$ (CGT) with different capping materials and thicknesses. The magnetic field was applied perpendicular to the substrate. From bottom to top the curves correspond to CGT without capping, capped with 5-nm-thick MgO, capped with 20-nm-thick NiO and capped with 50-nm-thick NiO. The curves are offset vertically to avoid overlap. (b) Optical micrograph of $Cr_2Ge_2Te_6$ flakes under different capping layers. The measured position and thickness of the flake is indicated by the line. Scale bar is 10 μm. The color for the frame of the micrograph corresponds to the color of the curves in (a).

sealed in a quartz tube. The mixture was then heated to 1050 °C and maintained at this temperature for 30 h. Then, the mixture was cooled down to 475 °C in a period of 10 days, after which the Ge-Te flux was removed by centrifuging at that temperature. The magnetic properties of the bulk crystals showed a T_C of 66 K as measured from the minimum of dM/dT curves (measured in a SQUID magnetometer with a magnetic field of 50 mT in the c-axis) in good agreement with previous reports.[2,4] Thin flakes of CGT were obtained by mechanically cleaving the synthetized crystals on top of silicon (Si) substrates (with 285 nm SiO_2 oxide on top of Si) using the Scotch tape method. Films of MgO or NiO were sputtered in a RF sputtering system at room temperature. To avoid unwanted heating during growth we restricted the MgO thickness to 5 nm. To investigate the possible mechanism of enhanced magnetism, we characterized magnetism of $Cr_2Ge_2Te_6$ with 6 different types of stacking. For three of them, we first cleaved $Cr_2Ge_2Te_6$ on silicon substrate and then sputtered an additional oxide capping layer, i.e. $Cr_2Ge_2Te_6$/NiO(50 nm), $Cr_2Ge_2Te_6$/NiO(20 nm), $Cr_2Ge_2Te_6$/MgO(5 nm). We note the thickness of the layer in the brackets. For other types, we cleaved $Cr_2Ge_2Te_6$ on NiO(20 nm) and MgO(5 nm). The last one is $Cr_2Ge_2Te_6$ on silicon substrate without additional layer. For the polar MOKE measurements, an Oxford MicrostatMO system was used in the Faraday configuration (light parallel to the magnetic field). A diode laser (635 nm) provided a linearly polarized laser beam that was intensity modulated with a mechanical chopper. The laser beam was then focused on the samples using a 0.6 NA 100X long working distance objective.

In Fig. 1(a), we show the hysteresis curves (Kerr rotation angle vs magnetic field) measured by MOKE at 7 K for CGT flakes with the capping layers of 20-nm-thick NiO, 50-nm-thick-NiO and 5-nm-thick MgO as well as for the flake without a capping layer. We choose the CGT flakes with similar thicknesses (13.7-nm-thick CGT for w/o capping, 12.5 nm for 20-nm-thick NiO, 14.0 nm for 50-nm-thick NiO, and 14.9 nm for 5-nm-thick MgO, measured by atomic force microscopy). The magnetic field is applied perpendicular to the substrate. As shown in Fig. 2(b), 5-nm-thick MgO did not change the color of the flakes and substrate as much as 20-nm-thick and 50-nm thick NiO did. This is due to a change in the optical thin film

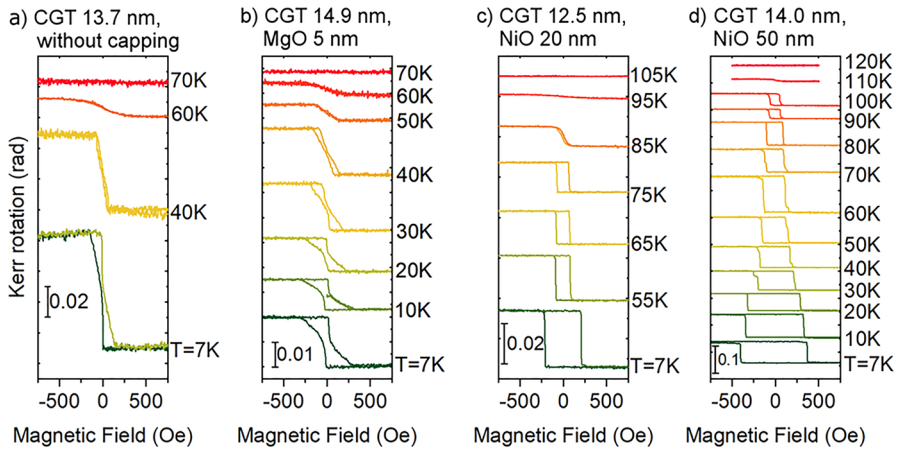

FIG. 2. Temperature evolution of magneto optical Kerr effect (MOKE) curves for (a) 13.7-nm-thick bare $Cr_2Ge_2Te_6$ (CGT), (b) 14.9-nm-thick CGT capped with 5-nm-thick MgO, (c) 12.5-nm-thick CGT capped with 20-nm-thick NiO, and (d) 14.0-nm-thick CGT capped with 50-nm-thick NiO.

interference effect of the transparent oxides. This effect depends on the index of refraction and the thicknesses of the transparent oxides or the optical path length. For 5 nm MgO the effect is weaker, and it appears as no apparent change in color. For 20 nm or 50 nm NiO thin films we have a higher change in optical path and can observe a complete change of color due to the interference. While the MOKE curve for MgO capped flake looks like the one for the control bare flake, the MOKE curve for NiO capped CGT shows a more rectangular loop with greater coercive field than the bare case. This indicates an increased perpendicular magnetic anisotropy (PMA) after deposition of NiO. Furthermore, a higher coercive field is observed for the thicker NiO thin film capped sample.

We have measured the hysteresis curves at elevated temperatures on the same flakes studied in Fig. 1. As shown in Fig. 2, it is revealed that the MOKE signal of 5 nm MgO capped CGT flake shows very similar temperature dependence as the bare case, but for 20 nm or 50 nm NiO capped flakes the hysteresis survives to higher temperatures than the case for bare CGT flakes. We determine the T_C as the midpoint between the temperature at which the MOKE curves indicate finite coercivity and the temperature at which the curve does not exhibit coercivity. We observed a T_C of 50 K for the case of the bare flake and 5 nm MgO capped CGT, a T_C of 90 K for the 20-nm-thick NiO capped sample and a T_C of 105 K for the 50-nm-thick NiO capped sample. The T_C of the bare flakes is consistent with reported T_C in bulk CGT.[2] The observed T_C for CGT/NiO corresponds to an increase of up to ~50 K for the flakes capped with a 50 nm NiO film. The same effect was reported for other thicknesses of NiO and wide range of thicknesses of CGT flakes in Ref. 12.

We measured MOKE on a thin CGT flake (6.9 nm) exfoliated on a 20-nm-thick NiO sputtered on Si substrate (with 285 nm SiO_2), thus, inverting the stacking order. In this configuration the CGT was not subject to the sputtering process of NiO. As shown in Fig. 3(a) no increased T_C is readily observed, in fact, the T_C is lower (~45 K) than bulk CGT which agrees with previous reports for thin CGT flakes.[2,12] Also, the shape of the hysteresis loop is different (lower coercive field), but we can attribute this to the dependence of the hysteresis loop on CGT thickness.[3,12,13] A similar behavior is observed in Fig. 3(b) for a 7.3-nm-thick CGT flake exfoliated on 5-nm-thick MgO sputter coated on Si substrate.

For further exploring the cause of the enhanced magnetism, we tried to observe exchange bias effect coming from antiferromagnetic NiO. While we succeeded to observe exchange bias effect in NiFe/NiO bilayer, we did not observe appreciable exchange bias in the MOKE curves for the NiO capped CGT samples as reported in other systems ($NiO/Ni_{81}Fe_{19}$[14]) even for samples where NiO was grown with an applied out-of-plane magnetic field during the sputtering. The role of exchange bias effect and magnetic proximity effect can be explored with further controlled experiment.[15]

Recently, increase of T_C was theoretically reported for tensile strained monolayer $Cr_2Ge_2Te_6$.[16,17] Also, in the case of the sister compound of $MCrS_2$ (where M is a monovalent metal), antiferromagnetic interactions between Cr atoms decreases with increase in-plane distance.[18] Such strain effects might be applicable to our case as wrinkle formation was observed for the 20 nm or 50 nm NiO capped flakes in contrast to no wrinkles in the 5 nm MgO capped samples. We speculate the wrinkles are due to thin film growth stress for the 20 nm and 50 nm NiO capping, and the absence of

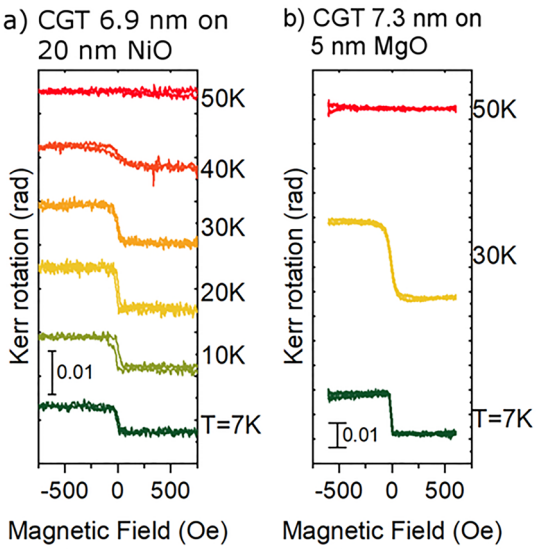

FIG. 3. Magneto optical Kerr effect (MOKE) curves at different temperatures for (a) 6.9 nm $Cr_2Ge_2Te_6$ (CGT) exfoliated on 20 nm NiO. (b) 7.3 nm CGT exfoliated on 5 nm of MgO.

wrinkles for 5 nm MgO capped samples could be related to a smaller intrinsic growth stress because of the smaller thickness of the oxide. Also, it is worth considering that MgO's Young modulus (230–320 GPa, calculated using ELATE online tool, Ref. 19) has been reported to be higher than NiO's (230–270 GPa, calculated using ELATE online tool with data from Materials Project online resource, Refs. 20 and 21) and one would expect easier deformation for the latter, which is consistent with wrinkling in NiO and not in MgO. We caution however that these properties are known to be dependent on the microstructure of the films and these were not analyzed here, thus making it hard to definitely conclude the role of the dissimilar elastic properties in our thin films. Other mechanisms as thermal expansion or contraction after growth are less likely to be the source of wrinkle formation as the sputtering of the thin films were performed at room temperature. Furthermore, we performed additional 20 nm NiO sputterings at higher temperatures (200 °C, 300 °C, 350 °C, 400 °C) which still showed wrinkles with decreasing occurrence for higher temperatures (300 °C and up), and increased signs of degradation for thin (less than 10 nm) CGT flakes as measured by Raman spectroscopy (see Fig. S1, in supplementary material) indicating that the temperature effect is not playing a significant role in wrinkle formation. Finally, the T_C enhancement and PMA enhancement are not always seen in all the NiO capped flakes (specifically, in flakes that have no wrinkles close to them, refer to Fig. S2). Due to these reasons, we performed a spatial dependent Raman characterization to probe strain close to wrinkled CGT flakes. Figure 4 shows spatial dependence of Raman spectrum on thin CGT/NiO flake with wrinkle structure, together with the spectrum without NiO. A thin CGT flake was chosen to avoid possible mixed Raman spectrum of strained and unstrained layers along the width of thicker flakes. We used HORIBA LabRAM HR-800 with 100X objective lens. The spectrum for the case of CGT without NiO layer is consistent with

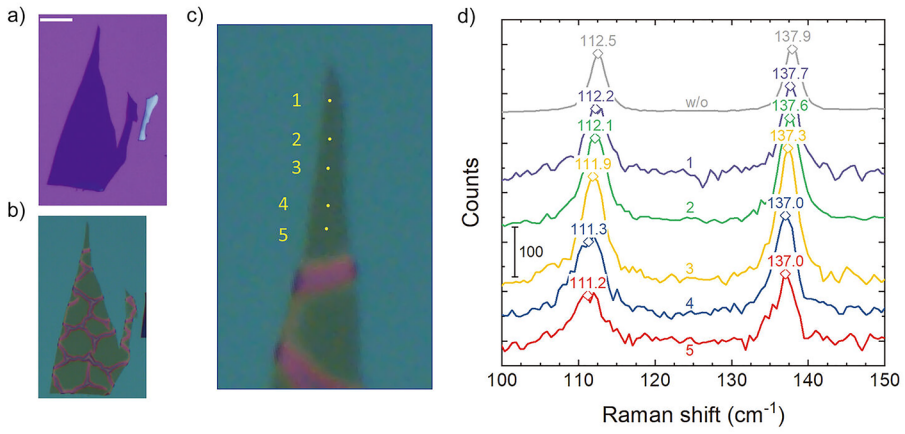

FIG. 4. Spatial variation of Raman spectrum for thin CGT/NiO flake with wrinkle structure. Optical micrograph for (a) CGT flake (b) CGT flake with NiO overlayer on Si substrate. Scale bar in (a) is 10 μm. (c) Optical micrograph with marked positions for Raman spectrum. (d) Raman spectrum of the five positions indicated in (c) together with a spectrum without NiO overlayer. Counts are shifted vertically for clarity. The fitted peak position is shown with diamond and number.

earlier report.[22] Importantly, the Raman spectrum of the thin flake (thickness ~4.5 nm) shows that the modes are shifted towards lower wavenumbers at positions closer to the wrinkle structure, which indicates that tensile strain is applied.[16,23] While the peak shift can be captured by eyes, we append the peak positions in Fig. 4(d), which is obtained by fitting Lorentzians after removing background using Labspec5 software (HORIBA Ltd.). It is worth noting that the wrinkle was not observed for the CGT flake exfoliated on top of NiO and MgO. Therefore, we conclude a plausible mechanism for the reported effects could be strain, whose presence is supported by the wrinkle formation.

In summary, we observed enhanced magnetism in the layered magnet CGT by interfacing it with 20-nm-thick or 50-nm-thick NiO films while no apparent modification is observed if the top oxide is 5-nm-thick MgO. A higher Curie temperature, reaching a T_C of 90 K for 20-nm-thick NiO capped CGT and 105 K for 50-nm-thick NiO capped CGT is reported and a stronger perpendicular magnetic anisotropy is observed in the NiO capped flakes when compared to bare flakes, while we did not observe noticeable enhancement of magnetism on flakes exfoliated on top of NiO and MgO. We have discussed the possible mechanism of increased Curie temperature from several points including measuring a spatial dependence of Raman spectrum in thin CGT flakes with NiO overlayer. The results suggest that interfacing CGT with oxides, especially with strain, can be used to greatly modify its magnetism, and push the magnetic properties closer to the desired point for technological applications.

SUPPLEMENTARY MATERIAL

See supplementary material for additional figures for Raman spectrum, optical micrographs and atomic force micrograph.

ACKNOWLEDGMENTS

We thank Dr. Lu for helpful discussion. This work was supported in part by NSF (ECCS1711332 and DMR1838513), by Advanced Institute for Materials Research (AIMR) under World Premier International Research Center Initiative (WPI) of MEXT, Japan, by the Center for Science and Innovation in Spintronics Research, by the Murata Foundation (M20_012), and by a Grant-in-Aid for Scientific Research from the Ministry of Education, Culture, Sports, Science and Technology (MEXT), JSPS KAKENHI (Grant Numbers 22H01896, and 20K14399). We also acknowledge technical help from AIMR common equipment unit.

AUTHOR DECLARATIONS

Conflict of Interest

The authors have no conflicts to disclose.

Author Contributions

A. E. LlacsahuangaAllcca: Conceptualization (equal); Data curation (equal); Formal analysis (equal); Investigation (equal); Methodology (equal); Writing – original draft (equal); Writing – review & editing (equal). **H. Idzuchi**: Conceptualization (lead); Data curation (equal); Formal analysis (equal); Funding acquisition (equal); Investigation (equal); Writing – original draft (equal); Writing – review & editing (lead). **X. C. Pan**: Resources (lead). **K. Tanigaki**: Resources (equal). **Y. P. Chen**: Conceptualization (equal); Funding acquisition (equal); Validation (equal); Writing – review & editing (equal).

DATA AVAILABILITY STATEMENTS

The data that support the findings of this study are available from the corresponding author upon reasonable request.

REFERENCES

[1] B. Huang, G. Clark, E. Navarro-Moratalla, D. R. Klein, R. Cheng, K. L. Seyler, D. Zhong, E. Schmidgall, M. A. McGuire, D. H. Cobden, W. Yao, D. Xiao, P. Jarillo-Herrero, and X. Xu, Nature **546**, 270 (2017).

[2] C. Gong, L. Li, Z. Li, H. Ji, A. Stern, Y. Xia, T. Cao, W. Bao, C. Wang, Y. Wang, Z. Q. Qiu, R. J. Cava, S. G. Louie, J. Xia, and X. Zhang, Nature **546**, 265 (2017).

[3] Z. Fei, B. Huang, P. Malinowski, W. Wang, T. Song, J. Sanchez, W. Yao, D. Xiao, X. Zhu, A. F. May, W. Wu, D. H. Cobden, J.-H. Chu, and X. Xu, Nat. Mater. **17**, 778 (2018).

[4]Z. Wang, T. Zhang, M. Ding, B. Dong, Y. Li, M. Chen, X. Li, J. Huang, H. Wang, X. Zhao, Y. Li, D. Li, C. Jia, L. Sun, H. Guo, Y. Ye, D. Sun, Y. Chen, T. Yang, J. Zhang, S. Ono, Z. Han, and Z. Zhang, Nat. Nanotechnol. **13**, 554 (2018).
[5]Y. Deng, Y. Yu, Y. Song, J. Zhang, N. Z. Wang, Z. Sun, Y. Yi, Y. Z. Wu, S. Wu, J. Zhu, J. Wang, X. H. Chen, and Y. Zhang, Nature **563**, 94 (2018).
[6]S. Jiang, L. Li, Z. Wang, K. F. Mak, and J. Shan, Nat. Nanotechnol. **13**, 549 (2018).
[7]B. Huang, G. Clark, D. R. Klein, D. MacNeill, E. Navarro-Moratalla, K. L. Seyler, N. Wilson, M. A. McGuire, D. H. Cobden, D. Xiao, W. Yao, P. Jarillo-Herrero, and X. Xu, Nat. Nanotechnol. **13**, 544 (2018).
[8]I. A. Verzhbitskiy, H. Kurebayashi, H. Cheng, J. Zhou, S. Khan, Y. P. Feng, and G. Eda, Nat. Electron. **3**, 460 (2020).
[9]N. Wang, H. Tang, M. Shi, H. Zhang, W. Zhuo, D. Liu, F. Meng, L. Ma, J. Ying, L. Zou, Z. Sun, and X. Chen, J. Am. Chem. Soc. **141**, 17166 (2019).
[10]L. Zhang, X. Huang, H. Dai, M. Wang, H. Cheng, L. Tong, Z. Li, X. Han, X. Wang, L. Ye, and J. Han, Adv. Mater. **32**, 2002032 (2020).
[11]C. Gong and X. Zhang, Science **363**, eaav4450 (2019).
[12]H. Idzuchi, A. E. Llacsahuanga Allcca, X. C. Pan, K. Tanigaki, and Y. P. Chen, Appl. Phys. Lett. **115**, 232403 (2019).
[13]A. Noah, H. Alpern, S. Singh, A. Gutfreund, G. Zisman, T. D. Feld, A. Vakahi, S. Remennik, Y. Paltiel, M. E. Huber, V. Barrena, H. Suderow, H. Steinberg, O. Millo, and Y. Anahory, Nano Lett. **22**, 3165 (2022).
[14]M. J. Carey and A. E. Berkowitz, Appl. Phys. Lett. **60**, 3060 (1992).
[15]M.-H. Phan, V. Kalappattil, V. O. Jimenez, Y. T. H. Pham, N. W. Mudiyanselage, D. Detellem, C.-M. Hung, A. Chanda, and T. Eggers, arXiv:2201.00479 (2022).
[16]B. H. Zhang, Y. S. Hou, Z. Wang, and R. Q. Wu, Phys. Rev. B **100**, 224427 (2019).
[17]X.-J. Dong, J.-Y. You, Z. Zhang, B. Gu, and G. Su, Phys. Rev. B **102**, 144443 (2020).
[18]A. V. Ushakov, D. A. Kukusta, A. N. Yaresko, and D. I. Khomskii, Phys. Rev. B **87**, 014418 (2013).
[19]R. Gaillac, P. Pullumbi, and F.-X. Coudert, J. Phys. Condens. Matter **28**, 275201 (2016), webpage: https://progs.coudert.name/elate/mp?query=mp-1265.
[20]A. Jain, S. P. Ong, G. Hautier, W. Chen, W. D. Richards, S. Dacek, S. Cholia, D. Gunter, D. Skinner, G. Ceder, and K. A. Persson, APL Mater. **1** (2013), 011002, Data from Materials Project online resource: https://materialsproject.org/materials/mp-19009#summary.
[21]M. De Jong, W. Chen, T. Angsten, A. Jain, R. Notestine, A. Gamst, M. Sluiter, C. K. Ande, S. Van Der Zwaag, J. J. Plata, C. Toher, S. Curtarolo, G. Ceder, K. A. Persson, and M. Asta, Sci. Data **2**, 1 (2015).
[22]Y. Tian, M. J. Gray, H. Ji, R. J. Cava, and K. S. Burch, 2D Mater. **3**, 025035 (2016).
[23]Y. Sun, R. C. Xiao, G. T. Lin, R. R. Zhang, L. S. Ling, Z. W. Ma, X. Luo, W. J. Lu, Y. P. Sun, and Z. G. Sheng, Appl. Phys. Lett. **112**, 072409 (2018).